



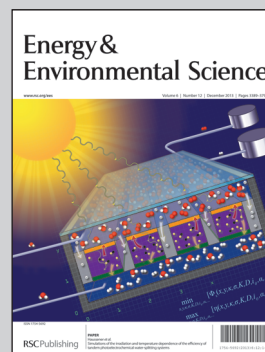
[View Article Online](#)  
[View Journal](#) | [View Issue](#)

## Showcasing research from Cheng-Wei Qiu's Laboratory, National University of Singapore, Singapore.

**Title:** Theoretical realization of an ultra-efficient thermal-energy harvesting cell made of natural materials

This paper targets the efficient usage of one important and vast energy source, i.e., thermal energy which can be collected from the environment. It presents a thermal cell for the very first time for harvesting heat energy with nearly 100% efficiency, only employing two types of bulky natural materials. It provides another alternative for utilizing clean energy.

### As featured in:



See Qiu *et al.*,  
*Energy Environ. Sci.*, 2013, **6**, 3537.

## COMMUNICATION

## Theoretical realization of an ultra-efficient thermal-energy harvesting cell made of natural materials

Tiancheng Han,<sup>a</sup> Jiajun Zhao,<sup>a</sup> Tao Yuan,<sup>a</sup> Dang Yuan Lei,<sup>b</sup> Baowen Li<sup>cd</sup> and Cheng-Wei Qiu<sup>\*a</sup>Cite this: *Energy Environ. Sci.*, 2013, **6**, 3537

Received 2nd May 2013

Accepted 8th July 2013

DOI: 10.1039/c3ee41512k

[www.rsc.org/ees](http://www.rsc.org/ees)

Three-dimensional devices capable of efficiently harvesting light energy or microwave radiation from arbitrary directions are still challenging to make due to the stringent requirement of inhomogeneous and extreme material parameters. This usually requires the use of metamaterials and results in time-consuming and complicated fabrication, narrow bandwidth performance and huge losses, which prevent these devices from being extended to large-scale energy-related applications. In this paper, we demonstrate that thermodynamic cells harvesting heat energy in three dimensions can be achieved by employing naturally available materials with constant thermal conductivity. Particularly, the thermal-energy harvesting efficiency of the proposed devices is independent of geometrical size and may achieve nearly 100% with tunable anisotropy, much superior to the concentrating devices reported so far. Theoretical analysis and numerical experiments validate the excellent performance of the advanced thermal cells. We further show that such thermal cells can be practically realized by using two naturally occurring conductive materials in a simplified planar geometry, which may open a new avenue for potential applications in solar thermal panels and thermal-electric devices.

## Introduction

Over the last few decades, much more attention has been paid to renewable energy. Solar energy is one of the alternative energies that have vast potential.<sup>1–3</sup> Solar cells play an important role allowing the collection of sunlight from a large area and focusing it on a smaller receiver or exit. Since conventional solar cells need a robust tracking system that is quite expensive,

## Broader context

Over the last few decades, much more attention has been paid to renewable energy. In addition to solar energy, another important energy source is thermal energy, which can be collected from the environment. Three-dimensional devices capable of efficiently harvesting thermal energy from arbitrary directions are still challenging to make due to the stringent requirement of inhomogeneous and extreme material parameters. This usually invokes the use of metamaterials and results in time-consuming and complicated fabrication, and huge losses, which prevent these devices from being extended to large-scale energy-related applications. In this paper, we demonstrate that thermodynamic cells harvesting heat energy in three dimensions can be achieved by employing naturally available materials with constant thermal conductivity. Particularly, the thermal-energy harvesting efficiency of the proposed devices is independent of geometrical size and may achieve nearly 100% with tunable anisotropy, much superior to the concentrating devices reported so far. We further show that such thermal cells can be practically realized by using two naturally occurring conductive materials in a simplified planar geometry, which may open a new avenue for potential applications in solar thermal panels and thermal-electric devices.

organic solar concentrators<sup>4,5</sup> and luminescent solar concentrators<sup>6</sup> have been proposed to reduce the cost with the price of lower efficiency. Based on nano-fabrication technology, absorption in nanostructured metal surfaces has been demonstrated with narrow bandwidth.<sup>7</sup> An optical black hole,<sup>8</sup> composed of an absorbing core and a gradient refractive index shell, has also been experimentally demonstrated in the microwave region with resonant metamaterials.<sup>9</sup> In addition to macroscopic concentrators,<sup>1–9</sup> plasmonics-based light harvesting devices have been studied, which function only at sub-wavelength scales.<sup>10–12</sup>

On the other hand, light-harvesting devices based on transformation optics,<sup>13,14</sup> capable of efficiently harvesting and focusing the incident light energy without severe reflection or absorption, are believed to play an important role in improving the energy-conversion efficiency of current solar cell devices in which high field-intensities are usually preferable.<sup>15–17</sup> In addition to solar energy, another important energy source is thermal

<sup>a</sup>Department of Electrical and Computer Engineering, National University of Singapore, 119620, Republic of Singapore. E-mail: [chengwei.qiu@nus.edu.sg](mailto:chengwei.qiu@nus.edu.sg); Fax: +65-6779-1103; Tel: +65-65162559

<sup>b</sup>Department of Applied Physics, The Hong Kong Polytechnic University, Hong Kong, China

<sup>c</sup>Department of Physics and Centre for Computational Science and Engineering, National University of Singapore, 117546, Republic of Singapore

<sup>d</sup>Center for Phononics and Thermal Energy Science, School of Physical Science and Engineering, Tongji University, 200092, Shanghai, China



energy, which can be collected from the environment. Transformation-optic method has also been extended to manipulate heat current.<sup>18,19</sup> However, practical realization of concentrating devices, particularly in three dimensions, often relies on the spatially varying material parameters comprising tensor components,<sup>15,16</sup> though the ideal parameters can be reduced partially.<sup>17</sup> Decoupling electric and magnetic effects, two-dimensional static electric concentrators based on resistor networks<sup>20</sup> and static magnetic concentrators based on superconductor-ferromagnetic metamaterials<sup>21</sup> have been demonstrated recently. Analogous to wavedynamics,<sup>15-17</sup> thermal concentrating devices reported so far are also facing similar serious bottlenecks, such as inhomogeneity,<sup>19</sup> which is challenging for the practical applications of three-dimensional thermal cells. Although a two-dimensional cylindrical concentrator made of latex rubber and processed silicone has recently been demonstrated in experiment and shown the fascinating ability to concentrate heat current, its concentrating efficiency is severely limited by the two-dimensional configuration, with an optimal value of  $\sim 12\%$ .<sup>22</sup> Thus, designing three-dimensional thermal concentrators with naturally available materials is of particular importance in enhancing the heat-harvesting efficiency in many energy-related applications.

In this paper, we establish the theoretical account and a general design road map for creating a realizable three-dimensional thermal cell made of natural conduction materials. Different from the previously studied concentrating devices in wave dynamics<sup>15-17</sup> and thermodynamics<sup>18,19</sup> obtained from rigorous transformation optics,<sup>13</sup> the proposed novel thermal cell is homogeneous in materials composition, and its performance is independent of the geometrical size but mainly dominated by the thermal-conduction anisotropy. By judiciously selecting the natural materials with strong thermal-conduction anisotropy or constructing composite materials of highly anisotropic thermal-conduction, the heat-concentrating efficiency of the studied cell can reach unity in an ideal situation. Due to the homogeneous response of the materials' conductivity in each individual direction, we further demonstrate that such advanced thermal cells can be realized in experiment through sophisticated spatial-arrangement of two naturally occurring conductive materials.

## Functional thermal-energy harvesting cell

### Concept design and numerical experiment

For a steady state without heat source, the thermal conduction equation can be written as  $\nabla \cdot (\kappa \nabla T) = 0$ , where  $\kappa$  is the thermal conductivity and  $T$  is the temperature. On the basis of the invariance of heat conduction equation under coordinate transformations,<sup>18</sup> the thermal conduction equation in the transformed space can be written as  $\nabla' \cdot (\vec{\kappa}' \nabla' T') = 0$ , through which we can obtain

$$\vec{\kappa}' = \frac{\mathbf{A}\kappa\mathbf{A}^T}{\det(\mathbf{A})}, \text{ with } \mathbf{A} = \frac{\partial(x', y', z')}{\partial(x, y, z)}. \quad (1)$$

The schematic diagram for the design of a three-dimensional thermal cell is shown in Fig. 1(a), where the spherical

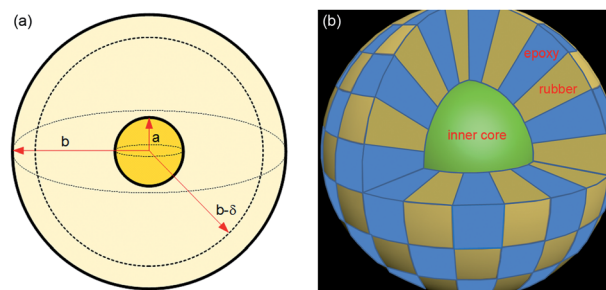


**Fig. 1** (a) Spatial coordinate transformation for the design of a homogeneous three-dimensional thermal cell. (b) The scheme for the realization of the homogeneous thermal cell in (a) with two naturally occurring materials.

region ( $0 \leq r \leq b - \delta$ ) and the shell region ( $b - \delta \leq r \leq b$ ) in virtual space are respectively mapped onto the inner core ( $0 \leq r' \leq a$ ) and coating ( $a \leq r' \leq b$ ) in real space. When  $\delta \rightarrow 0$ , the resulting thermal cell then consists of two parts:

For  $0 \leq r' \leq a$  (inner core):

$$\kappa'_r = \kappa'_\theta = \kappa'_\phi = b/a \quad (2a)$$

For  $a \leq r' \leq b$  (coating):

$$\kappa'_r \rightarrow \infty, \kappa'_t = \kappa'_\theta = \kappa'_\phi \rightarrow 0 \quad (2b)$$

Because the thermal conductivity of the inner core is homogeneous and isotropic, we then mainly focus on the conductivity of the coating shell. We may set  $\kappa'_r = 2^n$  and  $\kappa'_t = 2^{-n}$ , which exactly satisfy eqn (2b) if  $n$  is large enough. Assuming  $n = 4$  ( $\kappa'_r = 16$  and  $\kappa'_t = 1/16$ ), Fig. 2(a) shows the temperature profile and the heat flux streamline of a homogeneous spherical concentrator with  $a = 0.1$  m and  $b = 0.4$  m. It is clear that nearly all of the heat flux in the region ( $0 \leq r \leq b$ ) is focused into the inner core ( $0 \leq r \leq a$ ) without any reflection and distortion. According to the above theoretical analysis, the thermal cell will function more and more perfectly with the increase of  $n$ . However, what will happen if one pushes  $n$  toward the other extreme, *i.e.*, decreasing  $n$ ? Fig. 2(b) shows the temperature profile and heat flux streamline of the thermal cell in Fig. 2(a) with  $n = 1$  ( $\kappa'_r = 2$

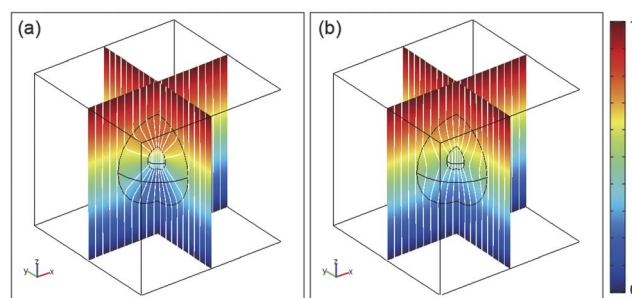


**Fig. 2** Normalized temperature profile and heat flux streamline for a spherical thermal cell with  $a = 0.1$  m and  $b = 0.4$  m. (a)  $n = 4$ . (b)  $n = 1$ . Streamlines of thermal flux are also represented by white color in the panel.



and  $\kappa'_t = 0.5$ ). It is very surprising that the thermal cell is still able to focus the heat current into the inner core without any reflection and distortion, which has never been achieved in wave dynamics<sup>15–17</sup> counterparts reported so far.

### Theoretical analysis

To explore the physical understanding of the interesting phenomenon that the thermal cell can function perfectly with arbitrary  $n$  ( $n > 1$ ), we introduce a rigorous theoretical analysis for such homogeneous thermal cells. The heat conduction equation in spherical coordinates is expanded as

$$\frac{\partial^2 T}{\partial r^2} + \frac{2}{r} \frac{\partial T}{\partial r} + \frac{\bar{\kappa}}{r^2 \sin \theta} \left[ \frac{\partial}{\partial \theta} \left( \sin \theta \frac{\partial T}{\partial \theta} \right) + \frac{1}{\sin \theta} \frac{\partial^2 T}{\partial \varphi^2} \right] = 0 \quad (3)$$

where  $\bar{\kappa} = 1$  for regions I ( $0 \leq r \leq a$ ) and III ( $r > b$ ),  $\bar{\kappa} = \kappa'_t/\kappa'_r = 2^{-2n}$  for region II ( $a \leq r \leq b$ ). To accord with the simulation setup, the boundary conditions are set as

$$T|_{z=\pm z_0} = \pm T_0, \quad \left. \frac{\partial T}{\partial x} \right|_{x=\pm x_0} = 0, \quad \left. \frac{\partial T}{\partial y} \right|_{y=\pm y_0} = 0. \quad (4)$$

Considering the symmetry in the  $\varphi$  direction and anti-symmetry in the  $z$  direction, the temperature field in the three regions can be respectively expressed as

$$T_1 = \sum_{m=1}^{\infty} A_{2m-1} r^{2m-1} P_{2m-1}(\cos \theta) \quad (5a)$$

$$T_2 = \sum_{m=1}^{\infty} [B_{2m-1} r^{l_m^+} + C_{2m-1} r^{l_m^-}] P_{2m-1}(\cos \theta) \quad (5b)$$

$$T_3 = \sum_{m=1}^{\infty} [D_{2m-1} r^{2m-1} + E_{2m-1} r^{-2m}] P_{2m-1}(\cos \theta) \quad (5c)$$

where  $l_m^{\pm} = -0.5 \pm 0.5 \sqrt{1 + 8\bar{\kappa}m(2m-1)}$  and  $P_m(x)$  denotes the Legendre function of degree  $m$ . The temperature and the normal component of the heat flux vector are continuous across the interfaces, which means

$$\begin{cases} T_1|_{r=a} = T_2|_{r=a}, \quad \kappa_1 \left. \frac{\partial T_1}{\partial r} \right|_{r=a} = \kappa'_r \left. \frac{\partial T_2}{\partial r} \right|_{r=a} \\ T_2|_{r=b} = T_3|_{r=b}, \quad \kappa'_r \left. \frac{\partial T_2}{\partial r} \right|_{r=b} = \kappa_3 \left. \frac{\partial T_3}{\partial r} \right|_{r=b} \end{cases} \quad (6)$$

According to the boundary condition  $T|_{z=\pm z_0} = \pm T_0$ , it is found that  $T_3$  is the linear distribution (which means  $E_{2m-1} = 0$ ) and one only needs to consider  $m = 1$ . Assuming  $\kappa_1 = \kappa_3 = 1$ , we can obtain

$$\frac{T_1}{T_3} = \left( \frac{a}{b} \right)^{l_1^+} \frac{b - b\kappa'_r l_1^-}{b - a\kappa'_r l_1^-} \quad (7)$$

Clearly, if  $n$  is large enough,  $T_1/T_3 \rightarrow b/a$ , which means that nearly 100% efficiency is achieved. To quantitatively examine the concentrating efficiency (CE) with variance of the heat conduction anisotropy (denoted by  $n$ ), we define

$$\text{CE}_{\text{SR}}^{3\text{D}} = |T|_{z=a} - T|_{z=-a}| / |T|_{z=b} - T|_{z=-b}| \quad (8)$$

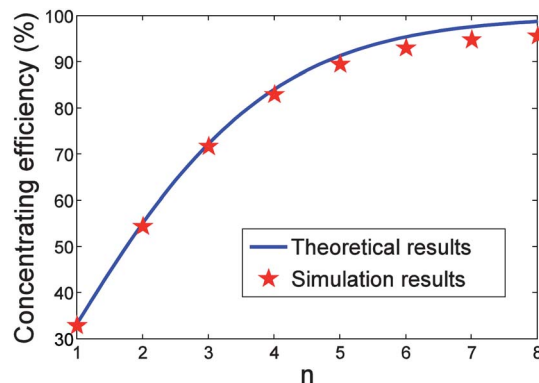


Fig. 3 Concentrating efficiency of the thermal cell with  $a = 0.1$  m and  $b = 0.4$  m as a function of  $n$ .

from simulation results and  $\text{CE}_{\text{TR}}^{3\text{D}} = T_1 a / T_3 b$  from theoretical results. Fig. 3 shows the calculated and simulated concentrating efficiency of the thermal cell designed in Fig. 2 as a function of  $n$ . Obviously, the theoretical results accord very well with the simulation results. The concentrating efficiency increases with  $n$ , and nearly reaches unity when  $n = 8$ . The larger the anisotropy, the higher the concentrating efficiency. On the one hand, this implies that it will be difficult to achieve maximum concentrating efficiency ( $\text{CE} \rightarrow 100\%$ ) with a small thermal-conduction anisotropy ( $n \rightarrow 0$ ). For engineering realization, we need to make a balance between the two quantities. On the other hand, the anisotropy-dependent concentrating efficiency also offers another parameter freedom to flexibly tune the performance of the device according to the requirements of practical applications.

### Recipe for experimental realization

We now turn to the theoretical recipe for realizing the proposed thermal cell *via* constructing a composite material, the heat conduction of which exhibits highly anisotropic response. Due to the homogeneous response of heat conduction in the proposed concentrator, the conduction anisotropy can be easily achieved through an alternating isotropic medium and in principle only two types of isotropic materials (medium A and medium B) are needed throughout. The heat conductivities of medium A and medium B are defined as  $\kappa_{A,B} = \kappa'_r \pm \sqrt{\kappa'_r{}^2 - \kappa'_r \kappa'_t}$ . For example, to obtain a homogeneous spherical cell with  $n = 2$  ( $\kappa'_r = 4$  and  $\kappa'_t = 0.25$ ), we can alternatively stack thermal epoxy ( $\kappa_A = 7.87$ ) and natural latex rubber ( $\kappa_B = 0.13$ ) along an azimuthal direction, as shown in Fig. 1(b). An alternation of  $N$  radially displaced epoxy and rubber wedges constitutes a natural discretization of the required anisotropic material, which functions as perfect as the ideal case with large  $N$ . According to Fig. 3, an ultra-efficient spherical cell with nearly 100% concentrating efficiency may be achieved by radially displacing copper and silica aerogel. It can be understood that if rubber in Fig. 1(b) is replaced with vacuum, the performance can be further improved a bit. Nevertheless, we used rubber taking into account the practicability in realistic experiments.



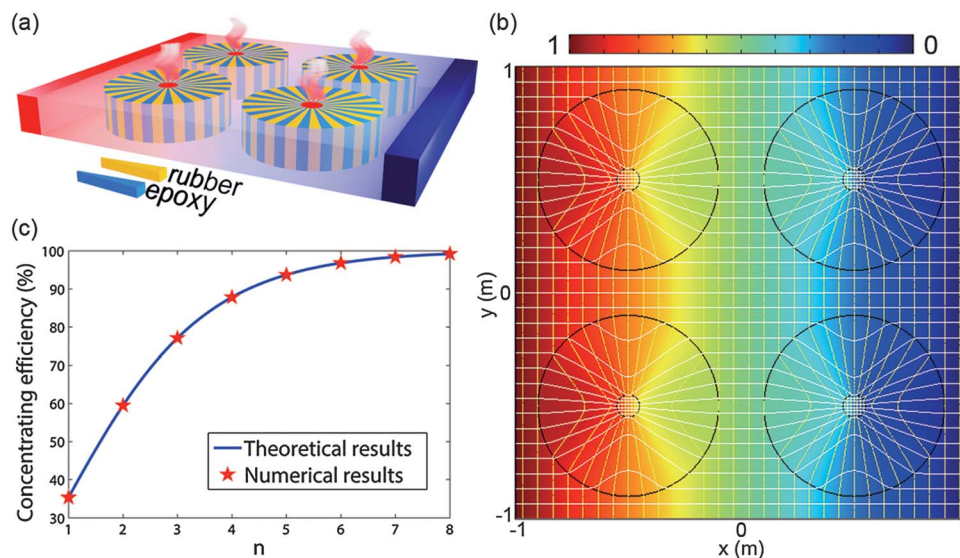


**Fig. 4** (a) The scheme for the realization of a thermal cluster with alternating naturally available materials, such as epoxy and rubber. (b) Top view of the temperature profile and heat flux streamline for the thermal cluster. Streamlines of thermal flux and isothermal are also represented by white and yellow colors in the panel, respectively. (c) Concentrating efficiency of the thermal cell in (b) as a function of  $n$ .

## Functional thermal-energy harvesting array

Next, we demonstrate a thermal array consisting of cylindrical thermal cells reduced from the three-dimensional case, as shown in Fig. 4(a). It should be noted that the advanced “homogeneity and tunable efficiency” property is still kept in the two-dimensional case. Since the conductivity of the inner core is always 1 in the two-dimensional case, we mainly focus on the coating region ( $a \leq r \leq b$ ) with  $\kappa'_r = 2^n$  and  $\kappa'_\theta = 2^{-n}$ . The thermal cell unit in Fig. 4(a) is created with  $a = 0.1$  m and  $b = 0.8$  m, and its conductivity in the coating region is set as  $\kappa'_r = 4$  and  $\kappa'_\theta = 0.25$ . The thermal array consists of identical individual thermal cells, each of which again can be realized by alternatively stacking the thermal epoxy ( $\kappa_A = 7.87$ ) and natural latex rubber ( $\kappa_B = 0.13$ ) along an azimuthal direction, as shown in Fig. 4(a). Fig. 4(b) shows the temperature profile of the thermal array, in which the deformation of the mesh formed by streamlines and isothermal values illustrates the excellent heat-concentrating performance. Therefore, a homogeneous and isotropic thermal array is simply achieved with naturally available materials.

Based on the theoretical analysis of the temperature distribution of the homogeneous cylindrical concentrator, we can obtain  $T_1/T_3 = (b/a)^{1-l}$  with  $l = \sqrt{\kappa'_\theta/\kappa'_r} = 2^{-n}$ . Clearly, we can obtain  $T_1/T_3 \rightarrow b/a$  if  $l \rightarrow 0$ , which means that nearly 100% efficiency is achieved. To quantitatively examine the concentrating efficiency of the homogeneous cylindrical thermal cell in Fig. 4(b), we calculate  $CE_{SR}^{2D} = |T|_{x=a} - T|_{x=-a}|/|T|_{x=b} - T|_{x=-b}|$  from simulation results and  $CE_{TR}^{2D} = T_1/T_3 b$  from theoretical results, as shown in Fig. 4(c). The theoretical results are in good agreement with the simulation results. As can be seen from Fig. 4(c), the concentrating efficiency up to 100% can be achieved when  $n = 8$ . This example shows that an ultra-efficient

thermal concentrator could be created, if a natural material with strong conduction anisotropy can be found or an effective material of highly anisotropic conduction can be constructed artificially.

## Conclusions

We have demonstrated three-dimensional thermal cells concentrating heat nearly perfectly with constant conductivity, which drastically facilitates the experimental realization and fabrication. The heat-concentrating performance of the thermal cell is mainly dominated by the heat-conduction anisotropy of the composition material, which could be easily constructed by periodically alternating two types of natural materials with isotropic conductivities. Particularly, the concentrating efficiency is independent of the geometrical size of the concentrator and nearly 100% efficiency could be achieved by judiciously selecting the natural materials, which has never been achieved in the previously studied concentrating devices.<sup>15–17,19</sup> The advanced thermal cell, composed of very simple materials, may find potential applications in devices such as solar thermal panels. We emphasize that the experimental demonstration of cylindrical concentrators reported recently<sup>22</sup> is a special case of our established general design road map.

## Acknowledgements

C.W.Q. acknowledges the Grant R-263-000-688-112 administered by National University of Singapore. T.C.H. also acknowledges the support from the Southwest University (SWU112035). D.Y.L. acknowledges the grants 1-ZVAL and 1-ZVAW administrated by the Hong Kong Polytechnic University.



## Notes and references

- 1 M. Romero and A. Steinfeld, *Energy Environ. Sci.*, 2012, **5**, 9234.
- 2 M. G. Debije and P. P. C. Verbunt, *Adv. Energy Mater.*, 2012, **2**, 12.
- 3 M. Bernardi, N. Ferralis, J. H. Wan, R. Villalon and J. C. Grossman, *Energy Environ. Sci.*, 2012, **5**, 6880.
- 4 M. J. Currie, J. K. Mapel, T. D. Heidel, S. Goffri and M. A. Baldo, *Science*, 2008, **321**, 226.
- 5 H. Hernandez-Noyola, D. H. Potterveld, R. J. Holt and S. B. Darling, *Energy Environ. Sci.*, 2012, **5**, 5789.
- 6 S. Tsoi, D. J. Broer, C. W. M. Bastiaansen and M. G. Debije, *Adv. Energy Mater.*, 2013, **3**, 337.
- 7 T. V. Teperik, *et al.*, *Nat. Photonics*, 2008, **2**, 299.
- 8 E. E. Narimanov and A. V. Kildishev, *Appl. Phys. Lett.*, 2009, **95**, 041106.
- 9 Q. Cheng, T. J. Cui, W. X. Jiang and B. G. Cai, *New J. Phys.*, 2010, **12**, 063006.
- 10 D. Y. Lei, A. Aubry, S. A. Maier and J. B. Pendry, *New J. Phys.*, 2010, **12**, 093030.
- 11 D. Y. Lei, A. Aubry, Y. Luo, S. A. Maier and J. B. Pendry, *ACS Nano*, 2011, **5**, 597.
- 12 D. Y. Lei, A. I. Fernandez-Dominguez, *et al.*, *ACS Nano*, 2012, **6**, 1380.
- 13 J. B. Pendry, D. Schurig and D. R. Smith, *Science*, 2006, **312**, 1780.
- 14 U. Leonhardt, *Science*, 2006, **312**, 1777.
- 15 M. Rahm, D. Schurig, D. A. Roberts, S. A. Cummer, D. R. Smith and J. B. Pendry, *Photon. Nanostruct. Fundam. Appl.*, 2008, **6**, 87.
- 16 A. D. Yaghjian and S. Maci, *New J. Phys.*, 2008, **10**, 115200.
- 17 W. Wang, L. Lin, J. Ma, *et al.*, *Opt. Express*, 2008, **16**, 11431.
- 18 T. Han, T. Yuan, B. Li and C.-W. Qiu, *Sci. Rep.*, 2013, **3**, 1593.
- 19 S. Guenneau, C. Amra and D. Veynante, *Opt. Express*, 2012, **20**, 8207.
- 20 W. X. Jiang, C. Y. Luo, H. F. Ma, Z. L. Mei and T. J. Cui, *Sci. Rep.*, 2012, **2**, 956.
- 21 C. Navau, J. Prat-Camps and A. Sanchez, *Phys. Rev. Lett.*, 2012, **109**, 263903.
- 22 S. Narayana and Y. Sato, *Phys. Rev. Lett.*, 2012, **108**, 214303.

